Journal of Computational Applied Mechanics 2026, 57(1): 27-40

DOI: 10.22059/jcamech.2025.402637.1615

RESEARCH PAPER

Computational Study of Micropolar Nanofluid Free Convection around a Circular Cylinder in a Porous Medium Subject to Magnetic and Electric Field Effects

Hamzeh Taha Alkasasbeh [a,*] Doha Mohammad Zghoul [a], Tariq A. Alarareh [b]

[a] *Department of Mathematics, Faculty of Science, Ajloun National University, P.O. Box 43, Ajloun 26810, Jordan.*
[b] *School of Mathematical Sciences, Universiti Sains Malaysia, Penang,11800, Malaysia*

Abstract

The integration of nanoparticles into base fluids markedly improves their thermal conductivity, thereby enhancing heat transfer performance. This enhancement has been extensively studied within engineering and industrial contexts. Likewise, the behavior of micropolar fluids under boundary layer convection has been well-characterized. However, research on micropolar nanofluids, particularly in the context of flow around circular cylinders, remains limited. This study investigates the free convection boundary layer flow of micropolar nanofluids around a circular cylinder. The governing equations are non-dimensionalized and converted into partial differential equations using similarity transformations. These equations are subsequently solved numerically via the Keller-Box method implemented in MATLAB. The effects of nanoparticle volume fraction and micropolar fluid parameters on flow behavior are systematically examined. Results demonstrate that increases in parameters such as magnetic field strength and porous medium permeability generally lead to elevated local wall temperatures and enhanced temperature profiles, although some reductions can occur under specific conditions. These findings highlight the critical influence of nanoparticle concentration and micropolar fluid characteristics on thermal performance, offering valuable insights for advancing research in fluid mechanics and heat transfer applications.

Keywords: Electric MHD; Nanofluid; Micropolar; Free Convection; Circular Cylinder; Porous Medium; Keller Box Method (KBM).

1. Introduction

Micropolar nanofluids are a specialized class of fluids that exhibit unique microstructural behaviours due to the presence of nanoparticles and micro-rotational effects. These fluids have garnered significant attention due to their enhanced rheological properties and potential applications across various fields (Muhammad et al [1]). The Natural convection of nanofluids or micropolar fluids on general bodies has been the subject of numerous investigations. Gorla and Takhar [2] looked into earlier thin bodies. However, Pop et al. [3] and Chiu and Chou [4] have also written on wavy surfaces. Furthermore, the natural convection flow from the curved surface with a micropolar fluid has been taken into consideration by Char and Chang [5]. It should be mentioned that Merkin [6] developed the viscous, free

* Corresponding author. Tel.: +962798662512.
E-mail address: alkasasbehh@gmail.com and alkasasbehh@anu.edu.jo

convective boundary layer flow issue with cylinder cross-section. Consequently, the problem of micropolar fluid (a non-Newtonian fluid) has been extended by Bhattacharyya and Pop [7] and Nazar et al.[8]. Many studies on free convection on a circular cylinder have been given based on that, including those [9-16]

Nanofluids are a new type of working fluids containing uniformly dispersed and suspended metallic or non-metallic nanoparticles. Due to its intriguing thermal properties and possible uses, this study issue has drawn the interest of numerous researchers since Choi's groundbreaking work Choi & Eastman [17]. The properties of nanofluids have been studied using two mathematical models: Buongiorno [18] and Tiwari-Das model. The Buongiorno method concentrates on thermophoresis and Brownian diffusion. Numerous writers, including Noreen et al.[19], Boulahia et al.[20], Qasim et al.[21] and Afridi and Qasim [22] have utilized this model in their investigation of nanofluid flow due to its significant significance. However, the Tiwari-Das model considered the volume fraction of nanoparticles rather than the effects of thermophoresis and Brownian motion. Many academics have used this approach to produce some intriguing results in recent years. Rahman et al.[23] examined the flow of water-based nanofluids past a wedge with a partial slide.

Thermal stratification on free convection in a square porous cavity filled with nanofluid was examined by Sheremet et al. [24]. Hussanan et al.[25] looked at the unsteady MHD flow of certain nanofluids via porous media over an accelerated vertical plate. The investigation of nanofluid flow in a porous channel with suction and chemical reaction was shown by Chen et al. [26]. A magnetic field on a water-based nanofluid containing Fe3O4 nanoparticles was examined by Sheikholeslami [27]. Using the same concept, Sheikholeslami [28]. examined the impact of coulomb forces on a suspended water-based nanofluid of Fe3O4 in a hollow with a moving wall. The natural convection flow of a micropolar nanofluid over a vertical plate was examined by Hussanan et al.[29]. They examined how oxide nanoparticles affected engine oil, kerosene, and water-based nanofluids. Using a micropolar fluid model, Hussanan et al. [30] also investigated the microstructure and inertial properties of a magnetite ferrofluid. The effects of natural convection on the boundary layer flow of Silver(Ag) and Graphene Oxide (GO) micropolar nanofluid around a solid sphere were emphasized by Swalmeh et al. [31].

The study of electric MHD (EHMD) nanofluids reveals significant potential for enhancing thermal management and heat transfer in industrial and technological applications. Continued research and development in this field are essential for optimizing their properties and expanding their practical applications. Daniel et al [32] presented the model electric MHD flow over stretching sheets or through channels, incorporating effects like thermal radiation, variable heat flux, Joule heating, viscous dissipation, and chemical reactions. These comprehensive approaches provide insights into how electric fields enhance velocity profiles while magnetic fields tend to reduce velocity but increase fluid temperature. Buongiorno's model and similar frameworks are used to describe nanofluid behaviour in EMHD. The interactions include effects of slip velocity, activation energy, and hybrid nanoparticles, improving fluid flow and heat transfer, this study by Shanmugapriya et al [33]. Abid et al [34] focused on practical applications highlighted include metallurgical engineering, machine building, and biomedical devices, emphasizing the relevance of EMHD nanofluids in industry. Mushahary and Ontela [35] studied the thermodynamic irreversibility, or entropy generation, associated with this complex flow system, focusing on the impacts of quadratic mixed convection under the influence of electromagnetic forces and porous media resistance. This study considers variable properties such as electrical conductivity and incorporates the couple-stress effects in the hybrid nanofluid to realistically model the fluid behaviour within the porous vertical channel environment. In a recent presentation, Alkasasbeh [36] discussed the modeling of Casson nanofluid flow on a stretching sheet with heat transfer: A study of Darcy-Forchheimer effects and electric MHD.

To the best of the author's knowledge, the flow of a Sodium Alginate (SA)-based micropolar nanofluid suspended with Silver (Ag) and Graphene Oxide (GO) nanoparticles over a heated horizontal circular cylinder has not yet been studied. To address this gap, the heat transfer flow of a micropolar nanofluid mixture containing copper and silver nanoparticles is analysed over a heated horizontal circular cylinder embedded in a porous medium under the influence of magnetic and electric fields. A similarity transformation is applied to convert the governing equations into a system of nonlinear ordinary differential equations, which are then solved using the implicit finite difference scheme known as the Keller-box method. The use of a micropolar nanofluid combining Silver and Graphene Oxide nanoparticles within the Sodium Alginate base fluid aims to enhance the thermal conductivity and improve overall heat transfer performance. This research provides insight into the complex interactions between magnetic fields, micropolar fluid dynamics, and nanoparticle dispersion, contributing to more efficient thermal management solutions in engineering applications.

2. Nomenclature

b	body force
B_0	Magnetic Field Strength, Wb
Cf	Local Skin Friction Coefficient,

c_p	Specific Heat Capacity, $Jkg^{-1}K^{-1}$
C_s	Coefficients of Space
Λ	Variable Permeability of Porous Medium,
ℓ	Gradient of velocity
M	Magnetic Parameter
m	Stretching Parameter
n	Carreau fluid index
Nu	Nusselt Number
Pr	Prandtl Number
Q	Heat Flux, Wm^{-2}
Re	Local Reynolds Number.
S_p	Heat Source/Sinks
T	Temperature,
u_w	Variable Shrinking Velocity, Ms^{-1}
V_w	Variable Velocity of Suction/Injection, Ms^{-1}
u	Velocity Component Along x-axis, Ms^{-1}
v	Velocity Component along Y-axis, Ms^{-1}
we	Williamson Parameter
μ	Dynamic Viscosity, $Kgm^{-1}s^{-1}$
k	Kinematic Viscosity, M^2s^{-1}
ρ	Density, Kgm^{-3}
σ	Electrical Conductivity, $A^2s^3kg^{-1}m^{-3}$
ϖ	Stream Function, $Kgm^{-1}s^{-1}$
τ	Shear Rate, $Kgm^{-1}s^{-2}$
ϵ	Ratio Parameter
ϕ	Nanoparticle Volume Fraction
Subscripts	
f	base fluid
hnf	Hybrid Nanofluid
w	Wall/Surface
∞	Ambient Environment

3. The problem description and governing equations

The cylinder is submerged in a steady, laminar, two-dimensional, incompressible, and viscous micropolar nanofluid. The nanofluid consists of Silver (Ag) and Graphene Oxide (GO) nanoparticles dispersed in a base fluid made of Sodium Alginate (SA). As illustrated in Figure 1, the surface temperature of the cylinder is maintained at a constant value at $T_w > T_\infty$, while the ambient temperature of the surrounding fluid remains uniform. The gravity vector, denoted by g, acts downward, opposite to the direction of the coordinate axis defined normal to the surface of the cylinder. Additionally, the system is subjected to a magnetic field B_0 of specified strength, which influences the fluid flow and heat transfer characteristics. The coordinate system employed in this analysis consists of two directions: the normal coordinate, measured perpendicular to the surface of the circular cylinder, and the angular coordinate, measured along the circumference of the horizontal cylinder starting from its lower stagnation point. This setup allows a detailed examination of the velocity and temperature fields around the cylinder.

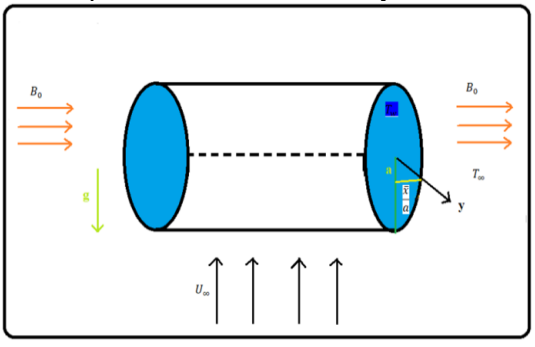

Fig 1: Physical model and coordinate system.

Here, the gravity acceleration vector, $\bar{g}$, can be written as follows in the x and y-directions:

$$g_x = -g\ sin\left(\frac{\bar{x}}{a}\right),\ g_y = g\ cos\left(\frac{\bar{x}}{a}\right), \tag{1}$$

The problem's governing PDEs, as determined by the aforementioned assumption and the Tiwari and Das nanofluid model are:

$$\frac{\partial \bar{u}}{\partial \bar{x}} + \frac{\partial \bar{v}}{\partial \bar{y}} = 0, \tag{2}$$

$$\bar{u}\frac{\partial \bar{u}}{\partial \bar{x}} + \bar{v}\frac{\partial \bar{u}}{\partial \bar{y}} = -\frac{1}{\rho_{nf}}\frac{\partial \bar{p}}{\partial \bar{x}} + \frac{(\mu_{nf}+k)}{\rho_{nf}}\left(\frac{\partial^2 \bar{u}}{\partial \bar{x}^2} + \frac{\partial^2 \bar{u}}{\partial \bar{y}^2}\right) + \left(\frac{\chi\rho_s\beta_s + (1-\chi)\rho_f\beta_f}{\rho_{nf}}\right) g(T - \quad T_\infty) sin\left(\frac{\bar{x}}{a}\right) + \frac{k}{\rho_{nf}}\left(\frac{\partial \bar{H}}{\partial \bar{y}}\right) + \frac{\rho_f\sigma_{nf}}{\rho_{nf}\sigma_f}(E_0 B_0 - B_0^2\bar{u}) - \frac{v_{nf}}{k^*}\bar{u}, \tag{3}$$

$$\bar{u}\frac{\partial T}{\partial \bar{x}} + \bar{v}\frac{\partial T}{\partial \bar{y}} = \frac{1}{Pr}\left(\frac{k_{nf}/k_f}{(1-\chi)+\chi(\rho c_p)_s/(\rho c_p)_f}\right)\left(\frac{\partial^2 T}{\partial x^2} + \frac{\partial^2 T}{\partial y^2}\right), \tag{4}$$

$$\bar{u}\frac{\partial \bar{H}}{\partial \bar{x}} + \bar{v}\frac{\partial \bar{H}}{\partial \bar{y}} = -\frac{\rho_f}{\rho_{nf}}K\left(2H + \frac{\partial \bar{u}}{\partial \bar{y}} - \frac{\partial \bar{v}}{\partial \bar{x}}\right) + \frac{\rho_f}{\rho_{nf}}\left(\emptyset(\chi) + \frac{K}{2}\right)\left(\frac{\partial^2 \bar{H}}{\partial \bar{x}^2} + \frac{\partial^2 \bar{H}}{\partial \bar{y}^2}\right), \tag{5}$$

corresponding to the following boundary conditions see (Nazar et al. [8]):

$$\bar{u} = \bar{v} = 0, T = T_w, \bar{H} = -n\frac{\partial \bar{u}}{\partial \bar{y}}\ at\ \bar{y} = 0,$$

$$\bar{u} \to 0, T \to T_\infty, H \to 0\ as\ \bar{y} \to \infty, \tag{6}$$

where $j = a^2/\sqrt{Gr}$ is the micro-inertia density, $\bar{u}$ and $\bar{v}$ are the velocity components along with the $\bar{x}$ and $\bar{y}$ axes. Additionally, the following definitions apply to the physical characteristics of nanofluid (nanofluid effects), which are $\beta_{nf}, \alpha_{nf}, \mu_{nf}\ \rho_{nf}, \phi_{nf}$, and k_{nf} (Sheremet et al. [24]):

$$(\beta\rho)_{nf} = (\chi(\beta\rho)_s + (1-\chi)(\beta\rho)_f)$$

$$(\beta)_{nf} = \frac{\left(\chi\beta_s\rho_s + (1-\chi)\,\beta_f\,\rho_f\right)}{\rho_{\ nf}}$$

$$(\mu)_{nf} = \frac{\mu_f}{(1-x)^{2.5}},$$

$$\left(\rho c_p\right)_{nf} = (\chi(\rho)_s + (1-\chi)\,(\rho c_p)_f),$$

$$\phi_{nf} = (\mu_{nf} + k\ /\ 2)J,$$

$$(\alpha)_{nf} = \frac{k_{nf}}{\left(\rho c_p\right)_{nf}},$$

$$(\rho)_{nf} = (\chi(\rho)_s + (1-\chi)(\rho)_f),$$

$$\frac{k_{nf}}{k_f} = \frac{(k_s+2k_f)-2x(k_f-k_s)}{(k_s+2k_f)+x(k_f-k_s)}, \tag{7}$$

where k_s, k_f and k_{nf} represent the solid, base fluid, and nanofluid's respective effective thermal conductivity; χ represents the nanoparticle volume fraction (or solid volume fraction) parameter; and $\left(\rho c_p\right)_{nf}, \left(\rho c_p\right)_f, \left(\rho c_p\right)_s$ represents the nanofluid, based fluid, and solid, respectively, in terms of heat capacity

The dimensionless variables are used to streamline computations where handling complex units of each variable and where parameters are required is no longer necessary. According to Nazar et al [8], the dimensionless variables in this problem are as follows:

$$x = \frac{\bar{x}}{a}, y = (Gr)^{(1/4)}\left(\frac{\bar{y}}{a}\right), \theta = \frac{T - T_\infty}{T_w - T_\infty},$$

$$u = (Gr)^{(-1/2)}\left(\frac{a\bar{u}}{v_f}\right), v = (Gr)^{(-1/4)}\left(\frac{a\bar{v}}{v_f}\right),$$

$$H = (Gr)^{(-3/4)}\left(\frac{a^2\bar{H}}{v_f}\right), p = (Gr)^{-1}\left(\frac{\bar{p}-p_\infty}{\rho_f\left(v_f^2/a^2\right)}\right), \tag{8}$$

such that the Grashof number is $Gr = g\,(\beta)_f\,(T_w - T_{\infty\_})\ a^3\ /\ v_f^2$ and the micro-inertia density for this boundary condition is $J = a^2\ /(Gr)^{(1/2)}$.

The following dimensionless form equations can be obtained by substituting the dimensionless variables (8) into equations (2)–(5):

$$\frac{\partial u}{\partial x} + \frac{\partial v}{\partial y} = 0\ , \tag{9}$$

$$u\ \frac{\partial u}{\partial x} + v\ \frac{\partial u}{\partial y} = -\frac{\partial p}{\partial x} + \frac{\rho_f}{\rho_{nf}}\ (\emptyset(\chi) + K)\frac{\partial^2 u}{\partial y^2} + \frac{1}{\rho_{nf}}\left(\chi\rho_s\left(\frac{\beta_s}{\beta_f}\right) + (1-\chi)\rho_f\right)\theta sinx + \frac{\rho_f}{\rho_{nf}}\ K\ \frac{\partial H}{\partial y} + \frac{\sigma_{nf}}{\rho_{nf}}\ M(E -$$

$u) - P_m\, u,$ (10)

$$u\frac{\partial\theta}{\partial x} + v\frac{\partial\theta}{\partial y} = \frac{1}{Pr}\left[\frac{k_{nf}/kf}{(1-\chi)+\chi(\rho c_p)_s/(\rho c_p)_f}\right]\frac{\partial^2\theta}{\partial y^2} \quad (11)$$

$$u\frac{\partial H}{\partial x} + v\frac{\partial H}{\partial y} = -\frac{\rho_f}{\rho_{nf}}K\left(2H + \frac{\partial u}{\partial y}\right) + \frac{\rho_f}{\rho_{nf}}\left(\emptyset(\chi) + \frac{K}{2}\right)\frac{\partial^2 H}{\partial y^2}, \quad (12)$$

where, $K = k/\rho_{nf}$ is micro-rotation parameter, $Pr = v_f/\alpha_f$ is the Prandtl number, $\emptyset(\chi) = (1-\chi)^{-2.5}$, magnetic parameter $M = \frac{\rho_f B_0^2}{\sigma_f}$, Electric parameter $E = \frac{E_0}{B_0 x}$. and Porous Medium parameter $P_m = \frac{V_{nf}}{k^*}$

The boundary condition (6) becomes

$$u = v = 0, \theta = 1, H = -\frac{1}{2}\frac{\partial u}{\partial y}\ at\ y = 0$$
$$u \to 0, \theta \to 0, H \to 0, as\ y \to \infty \quad (13)$$

The non-dimensional stream function ψ was defined as follows in order to reduce the non-dimensional system (9) to (12), which is related to the boundary conditions (13)

$$\psi = xf(x,y), \theta = \theta(x,y), H = xh(x,y), \quad (14)$$

where ψ is the stream function defined as

$$u = \frac{\partial\psi}{\partial y}\ and\ v = -\frac{\partial\psi}{\partial x}, \quad (15)$$

The continuity equation (9) is satisfied by this. Thus, equations (10) through (12) become into

$$\frac{\rho_f}{\rho_{nf}}(\emptyset(\chi) + K)\frac{\partial^3 f}{\partial y^3} + f\frac{\partial^2 f}{\partial y^2} - \left(\frac{\partial f}{\partial y}\right)^2 + \frac{1}{\rho_{nf}}\left(\chi\rho_s\left(\frac{\beta_s}{\beta_f}\right) + (1-\chi)\rho_f\right)\frac{\sin x}{x}\theta + \frac{\rho_f}{\rho_{nf}}K\frac{\partial h}{\partial y} + \frac{\sigma_{nf}}{\rho_{nf}}M\left(E - \frac{\partial f}{\partial y}\right) - P_m\frac{\partial f}{\partial y} = x\left(\frac{\partial f}{\partial y}\frac{\partial^2 f}{\partial x\partial y} - \frac{\partial f}{\partial x}\frac{\partial^2 f}{\partial y^2}\right), \quad (16)$$

$$\frac{1}{Pr}\left(\frac{k_{nf}/k_f}{(1-\chi)+\chi(\rho c_p)_s/(\rho c_p)_f}\right)\frac{\partial^2\theta}{\partial y^2} + f\frac{\partial\theta}{\partial y} = x\left(\frac{\partial f}{\partial y}\frac{\partial\theta}{\partial x} - \frac{\partial f}{\partial x}\frac{\partial\theta}{\partial y}\right), \quad (17)$$

$$\frac{\rho_f}{\rho_{nf}}\left(\emptyset(\chi) + \frac{K}{2}\right)\frac{\partial^2 h}{\partial y^2} + f\frac{\partial h}{\partial y} - \frac{\partial f}{\partial y}h - \frac{\rho_f}{\rho_{nf}}K\left(2h + \frac{\partial^2 f}{\partial y^2}\right) = x\left(\frac{\partial f}{\partial y}\frac{\partial h}{\partial x} - \frac{\partial f}{\partial x}\frac{\partial h}{\partial y}\right), \quad (18)$$

and boundary conditions become

$$f = \frac{\partial f}{\partial y} = 0, \theta = 1, h = -\frac{1}{2}\frac{\partial^2 f}{\partial y^2}\ at\ y = 0,$$
$$\frac{\partial f}{\partial y} \to 0, \theta \to 0, h \to 0\ as\ y \to \infty. \quad (19)$$

These equations can be observed to decrease to the following ordinary differential equations near the lower stagnation point of the cylinder $(x \approx 0)$.

$$\frac{\rho_f}{\rho_{nf}}(\emptyset(\chi) + K)f''' + ff'' - (f')^2 + \frac{1}{\rho_{nf}}\left(\chi\rho_s\left(\frac{\beta_s}{\beta_f}\right) + (1-\chi)\rho_f\right)\theta + \frac{\rho_f}{\rho_{nf}}Kh' + \frac{\sigma_{nf}}{\rho_{nf}}M(E - f') - P_m f' = 0 \quad , \quad (20)$$

$$\frac{1}{Pr}\left(\frac{k_{nf}/k_f}{(1-\chi)+\chi(\rho c_p)_s/(\rho c_p)_f}\right)\theta'' + f\theta' = 0\ , \quad (21)$$

$$\frac{\rho_f}{\rho_{nf}}\left(\emptyset(\chi) + \frac{K}{2}\right)h'' + fh' - \frac{\partial f}{\partial y}h - \frac{\rho_f}{\rho_{nf}}K(2h + f'') = 0, \quad (22)$$

The boundary conditions become

$$f(0) = f'(0) = 0, \theta(0) = 1, h(0) = -\frac{1}{2}f''(0)\ as\ y = 0, \quad (23)$$

The physical quantities of importance are the Nusselt number Nu and the local skin friction coefficient C_f which can be expressed as follows:

$$Cf = \frac{Gr^{-3/4}a^2}{\mu_f v_f}\tau_w, \quad Nu = \frac{aGr^{1/4}}{k_f(T_w - T_\infty)}q_w, \quad (24)$$

Where

$$\tau_w = \left(\mu_{nf} + \frac{k}{2}\right)\left(\frac{\partial\bar{u}}{\partial\bar{y}}\right)_{\bar{y}=0}, q_w = -k_{nf}\left(\frac{\partial T}{\partial\bar{y}}\right)_{\bar{y}=0}. \quad (25)$$

Applying the boundary conditions (13) and non-dimensional variables (8), the local skin friction coefficient C_f and Nusselt number Nu become

$$Cf = \left(\emptyset(\chi) + \frac{K}{2}\right)x\frac{\partial^2 f}{\partial y^2}(x,0), \quad Nu = -\frac{k_{nf}}{k_f}\left(\frac{\partial\theta}{\partial y}\right)(x,0). \quad (26)$$

4. The numerical method and validation

This section outlines the Keller-Box method, a numerical technique originally developed by Keller and Bramble [37], which is highly efficient and well-suited for solving convective boundary layer flow problems. In this study, the method was implemented following the approaches described by Na [38], Cebeci and Bradshaw [39], and Cousteix [40]. The Keller-Box method offers several notable advantages: it is unconditionally stable, provides second-order accuracy, and has demonstrated effectiveness in solving boundary layer problems for over three decades.

i. The computational procedure of the Keller-Box method, as applied in this work, consists of the following five key steps:
ii. Reduction of Order: The system of higher-order governing partial differential equations is transformed into a larger system of first-order equations.
iii. Discretization: The first-order equations are discretized using central difference approximations on a staggered (box) grid, which is a hallmark of this method and contributes to its second-order accuracy.
iv. Linearization: The resulting nonlinear algebraic system is linearized using Newton's method (or a modified Newtonian iteration).
v. Block-Matrix Formulation: The linearized equations are organized into a structured block-tridiagonal matrix system.
vi. Solution: The block-tridiagonal system is efficiently solved using the algorithm of LU decomposition.

The flow chart of the methodology is displayed in Figure 2. The ordinary differential equations (ODE) plus the boundary conditions are to be solved with this method, which is not a straightforward approach.

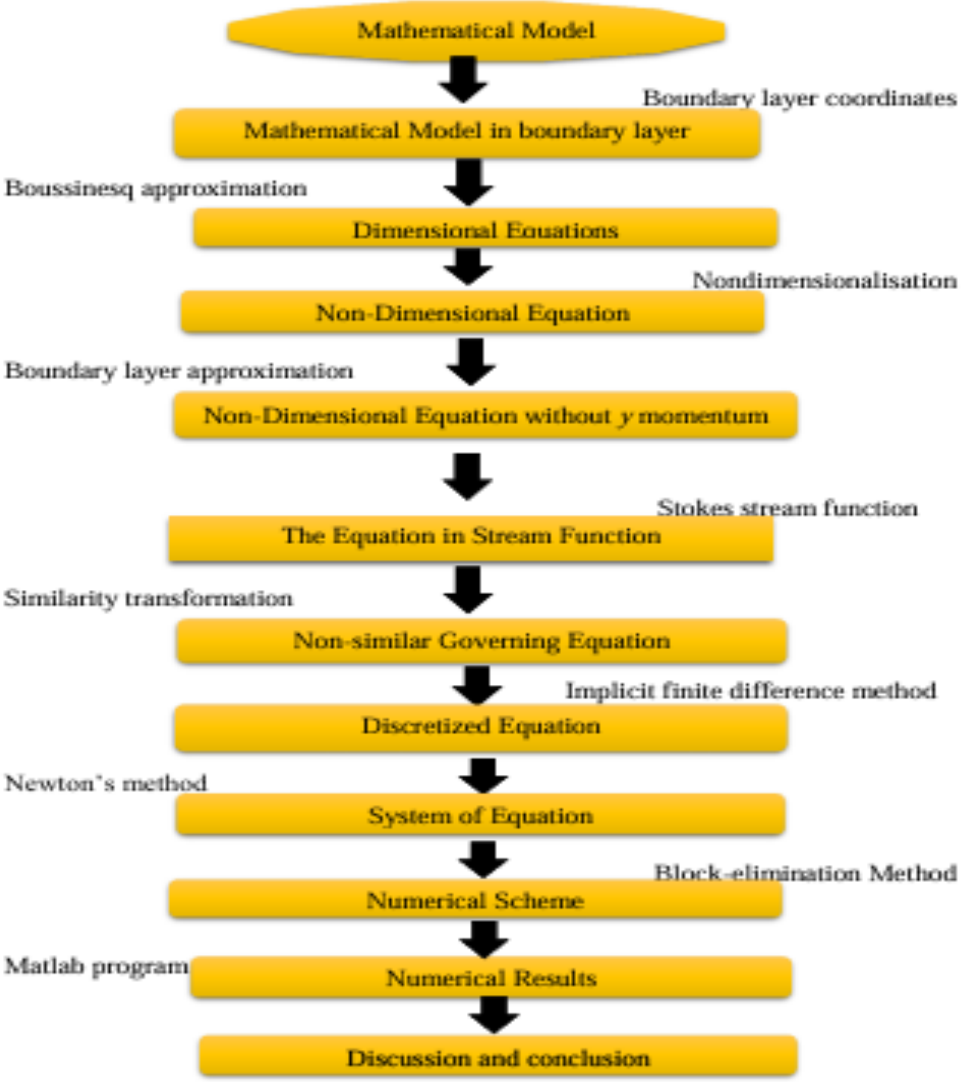

Fig 2: Flow chart of KBM method.

5. Results and Analysis

In order to generate graphical and numerical results about the behavior of a micropolar nanofluid based on Sodium Alginate and the effects of meaningfully related parameters on temperature, skin friction coefficient, velocity, and local Nusselt number, this section uses MATLAB to perform numerical computations. After that, the findings are carefully reviewed and talked about. The following range of parameters has been considered for the computational simulations: nanoparticles volume fraction ($0.1 \leq \chi \leq 0.2$), and magnetic parameter ($M > 0$).

Table 1 shows the thermophysical characteristics of the base fluid, Sodium Alginate (SA), and the nanoparticles Silver (Ag) and Graphene Oxide (GO) employed in this investigation. SA attributes include density (ρ), specific heat capacity (C_p), thermal conductivity (K), thermal expansion coefficient (β), electrical conductivity (σ), and (Pr) Prandtl number. These factors are crucial in defining the heat transfer and flow properties of the micropolar nanofluid. Notably, the high thermal conductivity of GO and Ag suggests their ability to improve the thermal performance of the base fluid.

Table 1: Thermo-physical properties of Silver (Ag), Graphene Oxide (GO) and Sodium Alginate (SA) as nanoparticle

Thermo-physical property	SA	Ag	GO
$\rho(kg/m^3)$	989	10,500	1800
$C_p(J/kgK)$	4175	235	717
$K(w/mK)$	0.6376	429	5000
$\beta \times 10^{-5}(K^{-1})$	99	1.89	28.4
$\sigma(s/m)$	2.6×10^{-4}	6.3×10^{7}	1.1×10^{-5}
Pr	6.5	_	_

Table 2: Comparison of local Nusselt number Nu with viscous Newtonian fluid, when $Pr = 1$ and $K = M = Pm = E = \chi = 0$.

x	Merkin [6]	Nazar et al. [8]	Swalmeh et al [16]	Present
0 °	0.4214	0.4214	0.4214	0.421410
30°	0.4161	0.4161	0.4163	0.416161
60°	0.4007	0.4005	0.4006	0.400625
90°	0.3745	0.3741	0.3744	0.374314
120°	0.3364	0.3355	0.3356	0.335991
150°	0.2825	0.2811	0.2811	0.281091
180^0	0.1945	0.1916	0.1913	0.191615

Table 3: Comparison of local skin friction coefficient Cf with viscous Newtonian fluid, when $Pr = 1$ and $K = M = Pm = E = \chi = 0$.

x	Merkin [6]	Nazar et al. [8]	Swalmeh et al [16]	Present
0 °	0.0000	0.0000	0.0000	0.0000
30°	0.4151	0.4148	0.4159	0.415214
60°	0.7558	0.7542	0.7538	0.755210
90°	0.9579	0.9545	0.9574	0.957725
120°	0.9756	0.9698	0.9743	0.975011
150°	0.7822	0.7740	0.7813	0.782014
180^0	0.3391	0.3265	0.3311	0.339014

Tables 2 and 3 show a high degree of agreement between the findings from this study and those from other published studies by Merkin [6], Nazar et al. [8] and Swalmeh et al [16], according to a thorough comparison. This robust association shows the consistency and dependability of the results in addition to validating the quality of the current mathematical modeling methodology and numerical procedure. Such consensus upholds the validity of the results reported in this study and increases trust in the approach used.

Figures 3 and 4 illustrate the variations of the local skin friction coefficient Cf and the Nusselt number Nu for different values of the magnetic parameter (M). It is clearly observed that both the skin friction coefficient and the Nusselt number decrease as the magnetic parameter increases. This reduction is primarily due to the restraining effect of the intensified magnetic field on the fluid flow. The stronger magnetic force acts as a damping mechanism, suppressing the velocity of the micropolar nanofluid and thereby inhibiting the natural convection process. As a result, both the momentum transfer near the cylinder surface (reflected in the skin friction coefficient) and the heat transfer rate (indicated by the Nusselt number) are diminished. These findings emphasize the significant influence of magnetic forces in controlling the fluid dynamics and thermal behavior around the heated cylinder, which has important implications for optimizing heat transfer in engineering systems involving magnetic fields..

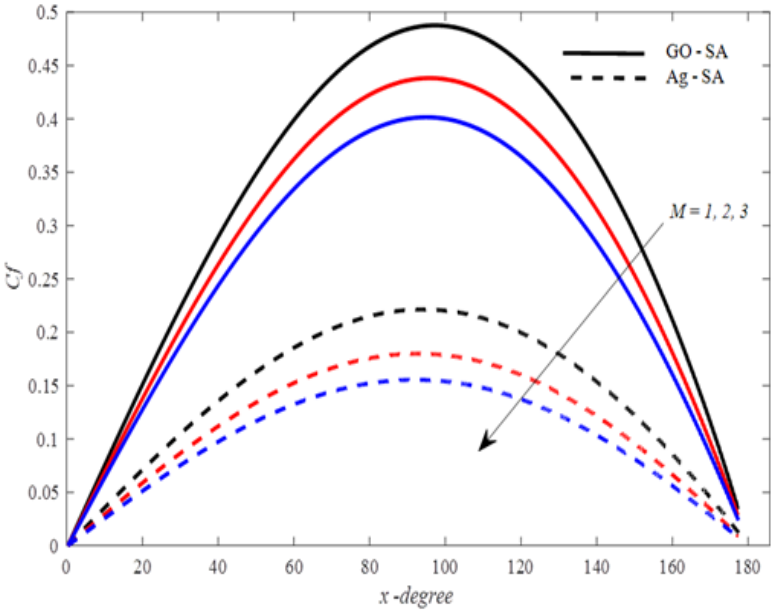

Fig3. Changes in M along with Cf

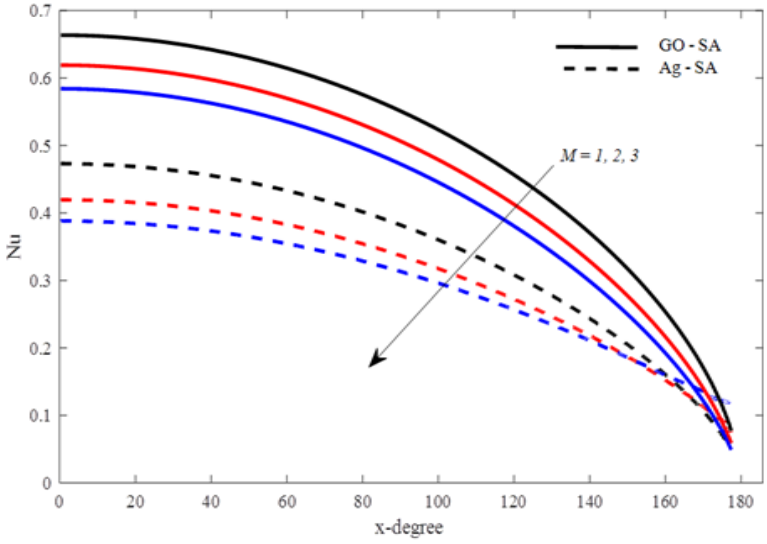

Fig4. Changes in M along with Nu

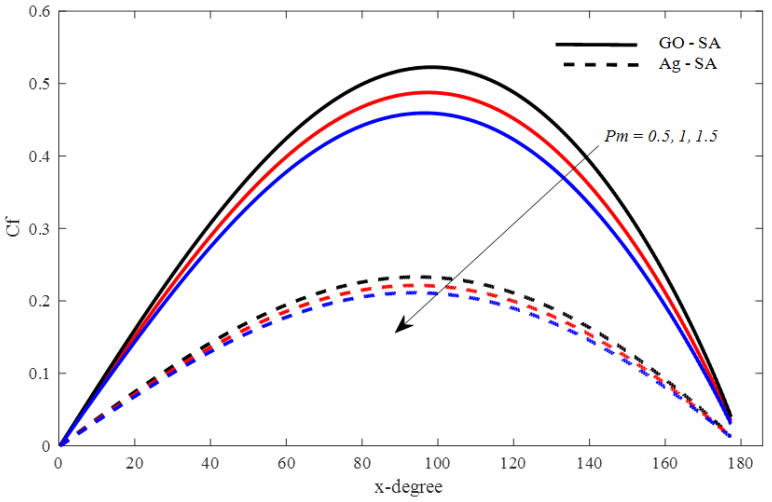

Fig 5. Changes in Pm along with Cf

Figures 5 and 6 present the graphical variations of the local skin friction coefficient Cf and the Nusselt number Nu for different values of the porous medium parameter. It is evident that both the skin friction coefficient and the Nusselt number decrease as the porous medium parameter Pm increases. This decline can be attributed to the increased resistance to fluid flow caused by the porous medium, which restricts the movement of the fluid. Consequently, the convection process is hindered, leading to reductions in both the skin friction coefficient and the heat transfer rate, as reflected by the lower Nusselt number. These results highlight the significant impact of the porous medium on diminishing fluid momentum and thermal transport near the surface of the cylinder.

Figures 7, 8, and 9 illustrate the impact of the magnetic parameter (M) on the velocity, angular velocity, and temperature profiles, respectively. It is observed that as the magnetic parameter increases, both the velocity and angular velocity profiles exhibit a noticeable rise. This behavior can be attributed to the influence of the magnetic field, which affects the momentum characteristics of the micropolar nanofluid flow. Conversely, the temperature profiles show a decreasing trend with increasing values of the magnetic parameter. This reduction in temperature is primarily due to the enhanced thermal conductivity resulting from a higher nanoparticle volume fraction in the nanofluid. The improved thermal conductivity facilitates more efficient heat dissipation, thereby lowering the overall temperature of the nanofluid.

These results highlight the significant role played by the magnetic field and nanoparticle concentration in controlling the flow dynamics and thermal behavior of the micropolar nanofluid around the heated horizontal cylinder.

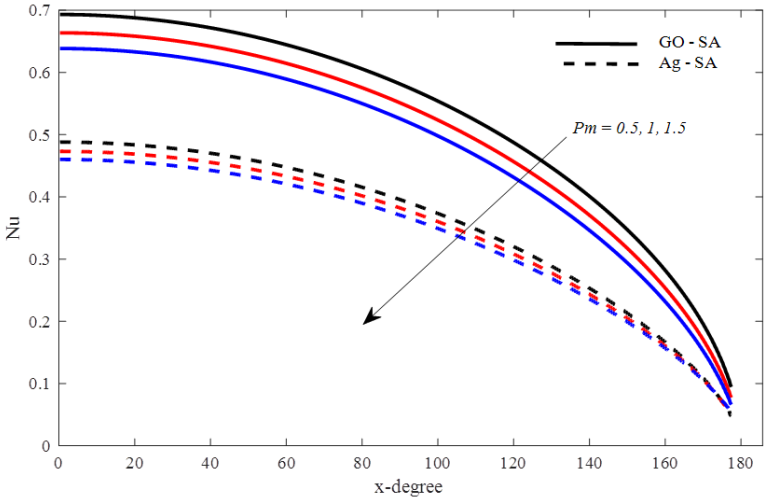

Fig 6: Changes in Pm along with Nu

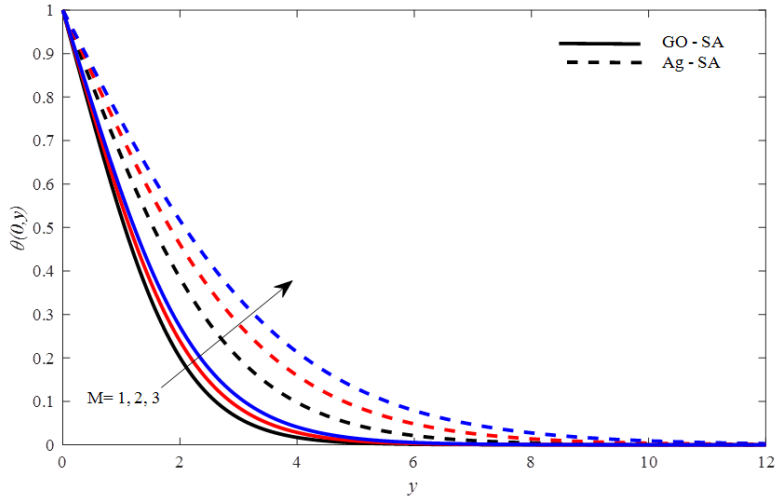

Fig7: Changes in *M* along with temperature

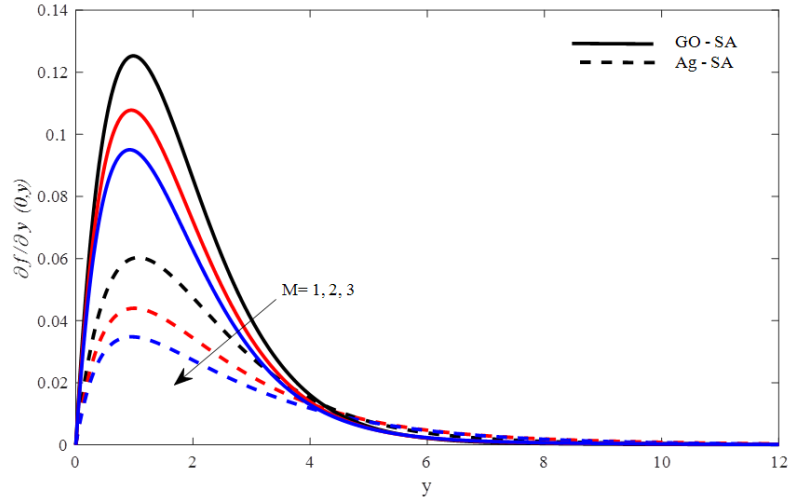

Fig 8: Changes in M along with velocity

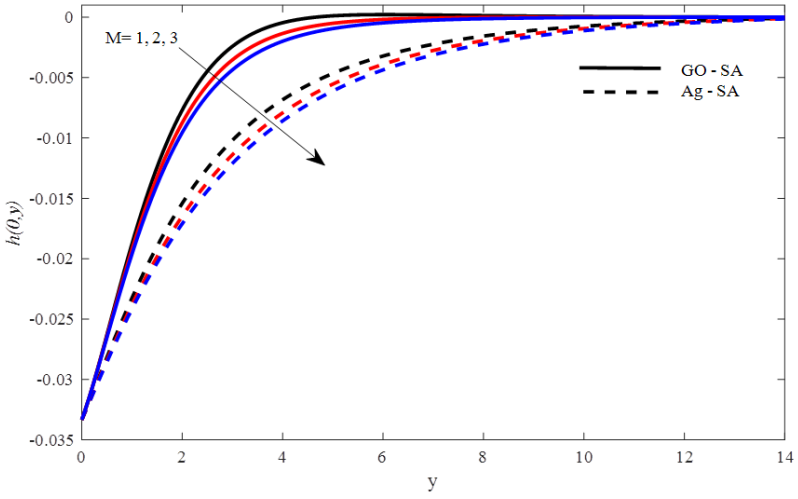

Fig 9: Changes in M along with angular velocity

Figures 10, 11, and 12 depict the influence of the porous medium parameter Pm on the velocity, angular velocity,

and temperature profiles, respectively. It is clearly observed that as the porous medium parameter Pm increases, both the velocity and angular velocity profiles show a corresponding increase. This can be explained by the enhanced permeability effects within Pm, which facilitate fluid motion and rotational behavior. In contrast, the temperature profiles exhibit a decreasing trend with an increase in the Pm. This reduction in temperature is primarily attributed to the increased nanoparticle volume fraction, which enhances the thermal conductivity of the nanofluid. As a result, the nanofluid is able to transfer heat more efficiently, leading to lower temperature levels within the fluid. These findings underscore the significant role that the characteristics of the porous medium and nanoparticle concentration play in modulating the flow and thermal performance of the micropolar nanofluid system.

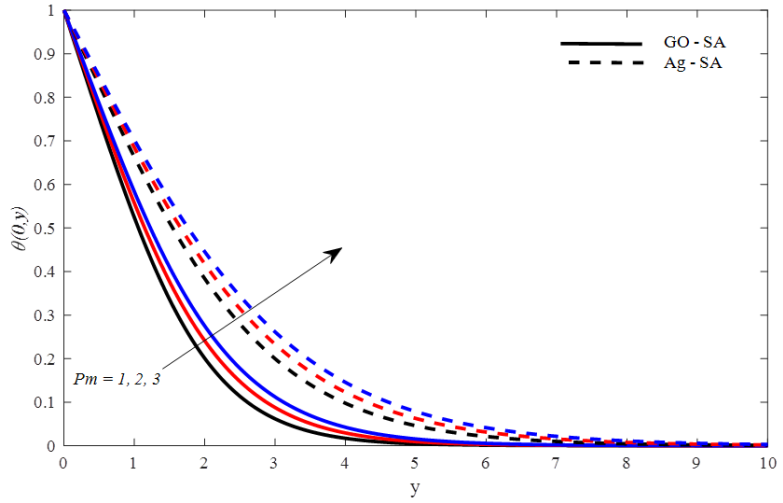

Fig 10: Changes in Pm along with temperature.

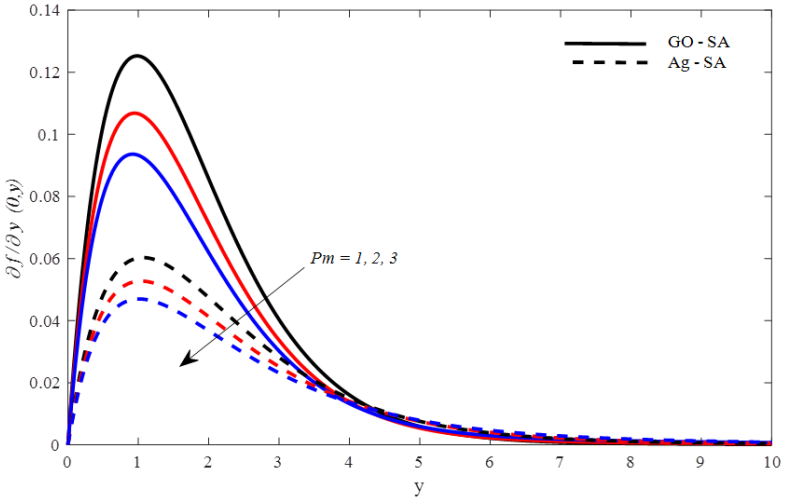

Fig 11: Changes in Pm along with velocity.

6. Conclusion:

The study focuses on fluids with broad applications in engineering and the physical world, along with the use of nanoparticles that have unique thermal properties to enhance heat transfer rates and flow characteristics of these fluids. Additionally, the pharmaceutical and food industries were considered in this study, which adds further value and significance to the research in engineering applications. This study also holds potential for future academic contributions. The results indicated the following:

- The skin friction coefficient (Cf) and Nusselt number (Nu) decrease as the magnetic parameter (M) increases.

- Both the skin friction coefficient (Cf) and Nusselt number (Nu) decline with an increase in the porous medium parameter (Pm).
- The porous medium restricts fluid movement similar to the magnetic field, thereby suppressing convection and lowering Cf and Nu values.
- Velocity and angular velocity profiles increase as the magnetic parameter (M) increases.
- The decrease is attributed to the enhanced thermal conductivity of the nanofluid with higher nanoparticle volume fraction, which improves heat dissipation and lowers temperature.
- Velocity and angular velocity profiles increase with increasing Pm.
- Similar to the magnetic parameter effect, this is due to increased thermal conductivity from higher nanoparticle volume fraction, reducing the nanofluid temperature.

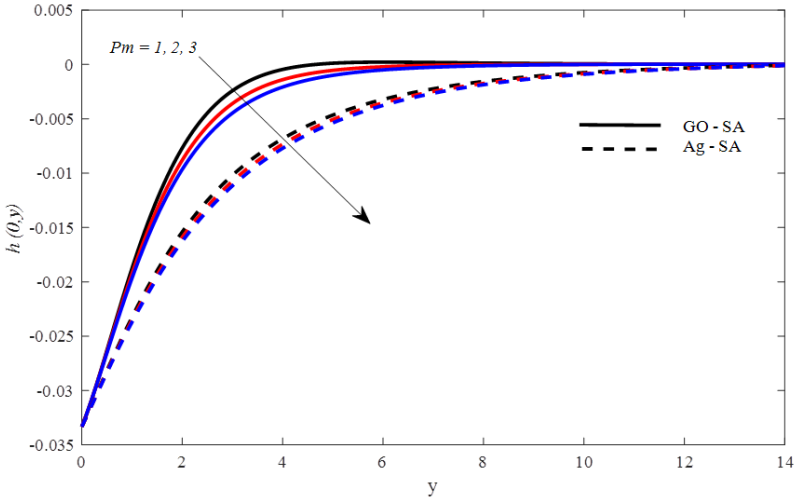

Fig 12: Changes in Pm along with angular velocity

Acknowledgement:

Author is grateful to acknowledge the Ajloun National University for providing the facilities support.

References

[1]. Muhammad, F, A Majeed, N Ijaz, K Barghout,N Abu-Libdeh, Exploration of heat transfer rate and chemically reactive bio-convection flow of micropolar nanofluid with gyrotactic microorganisms, *BioNanoScience,* Vol. 14, No. 2, pp. 1141-56, 2024.

[2]. Gorla, RSR,H Takhar, Free convection boundary layer flow of a micropolar fluid past slender bodies, *International journal of engineering science,* Vol. 25, No. 8, pp. 949-62, 1987.

[3]. Pop, I, H Takhar,M Kumari, Free convection about a vertical wavy surface with prescribed surface heat flux in a micropolar fluid, *Technische Mechanik-European Journal of Engineering Mechanics,* Vol. 18, No. 4, pp. 229-37, 1998.

[4]. Chiu, C-P,H-M Chou, Free convection in the boundary layer flow of a micropolar fluid along a vertical wavy surface, *Acta Mechanica,* Vol. 101, No. 1, pp. 161-74, 1993.

[5]. Char, M-I,C-L Chang, Laminar free convection flow of micropolar fluids from a curved surface, *Journal of Physics D: Applied Physics,* Vol. 28, No. 7, pp. 1324, 1995.

[6]. Merkin, J, Free convection boundary layers on cylinders of elliptic cross section, *ASME Journal of Heat Transfer,* Vol. 99, pp. 453-7, 1977.

[7]. Bhattacharyya, S,I Pop, Free convection from cylinders of elliptic cross-section in micropolar fluids, *International journal of engineering science,* Vol. 34, No. 11, pp. 1301-10, 1996.

[8]. Nazar, R, NS Amin,I Pop, Free convection boundary layer on an isothermal horizontal circular cylinder in a micropolar fluid, in *Proceeding of,* Begel House Inc., pp.

[9]. Mansour, M, M El-Hakiem,S El Kabeir, Heat and mass transfer in magnetohydrodynamic flow of micropolar fluid on a circular cylinder with uniform heat and mass flux, *Journal of Magnetism and Magnetic Materials,* Vol. 220, No. 2-3, pp. 259-70, 2000.

[10]. Mahfouz, F, Transient free convection from a horizontal cylinder placed in a micropolar fluid, *Heat and mass transfer,* Vol. 39, No. 5, pp. 455-62, 2003.

[11]. Chang, C-L, Numerical simulation for natural convection of micropolar fluids flow along slender hollow circular cylinder with wall conduction effect, *Communications in Nonlinear Science and Numerical Simulation,* Vol. 13, No. 3, pp. 624-36, 2008.

[12]. Abu-Nada, E, K Ziyad, M Saleh,Y Ali, Heat transfer enhancement in combined convection around a horizontal cylinder using nanofluids, 2008.

[13]. Abbas, N, S Saleem, S Nadeem, A Alderremy,A Khan, On stagnation point flow of a micro polar nanofluid past a circular cylinder with velocity and thermal slip, *Results in Physics,* Vol. 9, pp. 1224-32, 2018.

[14]. Mustafa, M, M Swalmeh, H Alkasasbeh,A Hussanan, Numerical Study of Mixed Convection Heat Transfer in Methanol based Micropolar Nanofluid about a Horizontal Circular Cylinder, 2019.

[15]. Qadan, H, H Alkasasbeh, N Yaseen, MZ Sawalmeh,S ALKhalafat, A Theoretical study of steady MHD mixed convection heat transfer flow for a horizontal circular cylinder embedded in a micropolar casson fluid with thermal radiation, *Journal of Computational Applied Mechanics,* Vol. 50, No. 1, pp. 165-73, 2019.

[16]. Swalmeh, MZ, HT Alkasasbeh, A Hussanan,M Mamat, Influence of micro-rotation and micro-inertia on nanofluid flow over a heated horizontal circular cylinder with free convection, *Theoretical and Applied Mechanics,* Vol. 46, No. 2, pp. 125-45, 2019.

[17]. Choi, SU,JA Eastman. Enhancing thermal conductivity of fluids with nanoparticles. Argonne National Lab.(ANL), Argonne, IL (United States), 1995.

[18]. Buongiorno, J, Convective transport in nanofluids, 2006.

[19]. Noreen, S, M Rashidi,M Qasim, Blood flow analysis with considering nanofluid effects in vertical channel, *Applied Nanoscience,* Vol. 7, No. 5, pp. 193-9, 2017.

[20]. Boulahia, Z, A Wakif,R Sehaqui, Finite volume analysis of free convection heat transfer in a square enclosure filled by a Cu-water nanofluid containing different shapes of heating cylinder, *Journal of Nanofluids,* Vol. 6, No. 4, pp. 761-8, 2017.

[21]. Qasim, M, Z Hayat Khan, I Khan,QM Al-Mdallal, Analysis of entropy generation in flow of methanol-based nanofluid in a sinusoidal wavy channel, *Entropy,* Vol. 19, No. 10, pp. 490, 2017.

[22]. Afridi, M,M Qasim, Comparative study and entropy generation analysis of Cu–H2O and Ag–H2O nanofluids flow over a slendering stretching surface, *Journal of Nanofluids,* Vol. 7, No. 4, pp. 783-90, 2018.

[23]. Rahman, M, M Al-Lawatia, I Eltayeb,N Al-Salti, Hydromagnetic slip flow of water based nanofluids past a wedge with convective surface in the presence of heat generation (or) absorption, *International Journal of Thermal Sciences,* Vol. 57, pp. 172-82, 2012.

[24]. Sheremet, MA, S Dinarvand,I Pop, Effect of thermal stratification on free convection in a square porous cavity filled with a nanofluid using Tiwari and Das' nanofluid model, *Physica E: Low-Dimensional Systems and Nanostructures,* Vol. 69, pp. 332-41, 2015.

[25]. Hussanan, A, I Khan, H Hashim, MK Anuar, N Ishak, NM Sarif,MZ Salleh, Unsteady MHD flow of some nanofluids past an accelerated vertical plate embedded in a porous medium, *Jurnal Teknologi (Sciences & Engineering),* Vol. 78, No. 2, 2016.

[26]. Chen, H, T Xiao,M Shen, Nanofluid flow in a porous channel with suction and chemical reaction using Tiwari and Das's nanofluid model, *Heat Transfer—Asian Research,* Vol. 46, No. 7, pp. 1041-52, 2017.

[27]. Sheikholeslami, M, Magnetic source impact on nanofluid heat transfer using CVFEM, *Neural Computing and Applications,* Vol. 30, No. 4, pp. 1055-64, 2018.

[28]. Sheikholeslami, M, Influence of Coulomb forces on Fe3O4–H2O nanofluid thermal improvement, *International Journal of Hydrogen Energy,* Vol. 42, No. 2, pp. 821-9, 2017.

[29]. Hussanan, A, MZ Salleh, I Khan,S Shafie, Convection heat transfer in micropolar nanofluids with oxide nanoparticles in water, kerosene and engine oil, *Journal of Molecular Liquids,* Vol. 229, pp. 482-8, 2017.

[30]. Hussanan, A, S Aman, Z Ismail, MZ Salleh,B Widodo, Unsteady natural convection of sodium alginate viscoplastic Casson based based nanofluid flow over a vertical plate with leading edge accretion/ablation, *Journal of Advanced Research in Fluid Mechanics and Thermal Sciences,* Vol. 45, No. 1, pp. 92-8, 2018.

[31]. Swalmeh, MZ, HT Alkasasbeh, A Hussanan,M Mamat, Heat transfer flow of Cu-water and Al2O3-water micropolar nanofluids about a solid sphere in the presence of natural convection using Keller-box method, *Results in Physics,* Vol. 9, pp. 717-24, 2018.

[32]. Daniel, YS, ZA Aziz, Z Ismail,F Salah, Double stratification effects on unsteady electrical MHD mixed convection flow of nanofluid with viscous dissipation and Joule heating, *Journal of applied research and technology,* Vol. 15, No. 5, pp. 464-76, 2017.

[33]. Shanmugapriya, M, R Sundareswaran,P Senthil Kumar, Heat and mass transfer enhancement of MHD hybrid nanofluid flow in the presence of activation energy, *International journal of chemical engineering,* Vol. 2021, No. 1, pp. 9473226, 2021.

[34]. Abid, A, A Azad,AA Bhuiyan, Enhancing radiative efficiency in MHD micropumps using plasma-infused hybrid bioconvective nanofluids for advanced radiative oncology at tertiary level, *Scientific Reports,* Vol. 13, No. 1, pp. 18452, 2023.

[35]. Mushahary, P,S Ontela, Entropy analysis of mixed convective electro-magnetohydrodynamic couple-stress hybrid nanofluid flow with variable electrical conductivity in a porous channel, *Physica Scripta,* Vol. 99, No. 11, pp. 115253, 2024.

[36]. Alkasasbeh, HT, Modeling the flow of casson nanofluid on a stretching sheet with heat transfer: A study of electric mhd and darcy-forchheimer effects, *Partial Differential Equations in Applied Mathematics,* Vol. 13, pp. 101109, 2025.

[37]. Keller, HB, *A new difference scheme for parabolic problems*, in: *Numerical solution of partial differential equations–II*, Eds., pp. 327-50: Elsevier, 1971.

[38]. Na, TY, 1980, *Computational methods in engineering boundary value problems*, Academic press,

[39]. Cebeci, T,P Bradshaw, 2013, *Physical and computational aspects of convective heat transfer*, Springer Science & Business Media,

[40]. Cousteix, TCJ,J Cebeci, Modeling and computation of boundary-layer flows, *Berlin, Germany: Springer*, 2005.